AGH Journal of Mining and Geoengineering • Vol. 36 • No. 2 • 2012

*Marian Branny *, Michał Karch *, Waldemar Wodziak *,*
*Janusz Szmyd **, Marek Jaszczur **, Remigiusz Nowak ***

AIR FLOW MEASUREMENTS THROUGH THE LABORATORY STAND OF THE CROSSING OF THE LONG WALL AND VENTILATION GALLERY FOR CFD CODE VALIDATION

1. Introduction

Computational fluid mechanics is currently one of the most popular methods of problem solution of fluid mechanics and physics. When applied to problems of the mining domain, this technique is applied to local tasks related to the ventilation of mines such as the ventilation of faces or of blind drifts. The subject of numerical modeling is two– or threedimensional air flows with the exchange of mass, momentum, and energy. One of the aims of the flow descriptions is to take into account the processes connected with the exchange of heat and inflow of gases from the strata and those ones emitted by working machines. In the researches on the 2D and 3D flow problems, models developed on the basis of computational fluid mechanics (CFD models) are applied. Generally, for the modeling of technical problems viscous models of turbulence are used. They are based on Reynolds averaging (RANS) and assume the existence of turbulent viscosity. With the use of these models in the studies [5, 6, 9] distributions of flow velocities and methane concentrations in mine faces have been analyzed and the authors [2, 3] have determined the velocity fields, temperatures, concentrations of methane and dust in the blind drifts. The main restriction of the practical application of the obtained results is the necessity of their experimental verification due to the fact that none of the developed turbulence models is universal. They involve several simplifying assumptions and for a particular problem such models should be verified experimentally.

* AGH University of Science and Technology, Faculty of Mining and Geoengineering, Krakow
** AGH University of Science and Technology, Faculty of Energy and Fuels, Krakow

In the article the results of experimental and numerical research on the air flow through the system of T-shaped ventilation ducts are presented. The laboratory model is a certain simplification of the working system of the intersection of the long wall with the ventilation gallery. The simplifications refer both to the geometry of the object (the cross-section of the workings is rectangular, hydraulically smooth walls, without elements as equipment of mining face or drifts) as well as flow conditions (without the air inflow from the goaf domain). The aim of the conducted research is an attempt to evaluate the accuracy with which numerical simulations map the real flow. The numerical simulation of the air flow for identical conditions as in the experiment has been carried out with the use of the FLUENT software.

2. Experimental setup

The experimental setup shown in Figure 1 consists of the inlet channel (final part of the long wall), the outlet channel (ventilation gallery) at the end of which a fan has been installed, and the cavity. The cross-section of channels are in size of 4.0×2.0 m whereas the length of the cavity equals to 5.0 m. The laboratory model was built in the geometric scale 1:10. If the examined flow is to reflect the conditions of the real one, the criteria of flow similarity must be met. For air is the flow medium in the model, the condition of the equality of Prandtl's number is fulfilled automatically. The equality of the Reynold's number in the model and the real object assures the flow criteria are similar. If the average velocity of air flow in the real object is assumed to be equal to 1m/s, the required flow velocity in the model is 10 m/s.

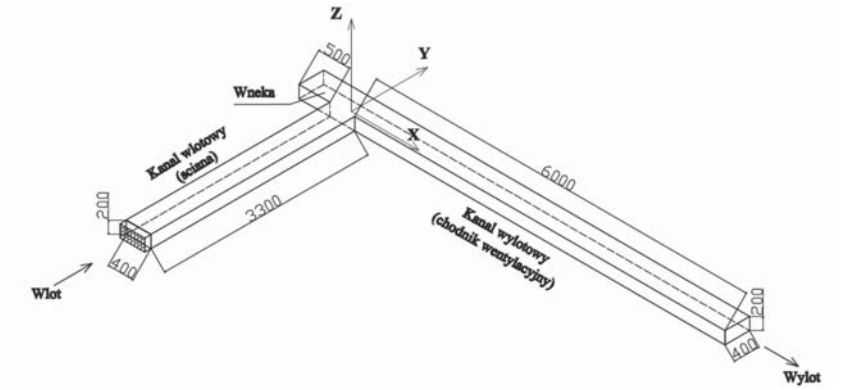

Fig. 1. Experimental set-up

Measurements of velocity fields have been carried out with the PIV method (*Particle Image Velocimetry*). It allows for a simultaneous determination of the velocity field in the whole examined domain. The velocity vectors are derived from sub-sections of the target area of the particle-seeded flow by measuring the movement of particles between two light pulses. The particles are illuminated with a double-pulse laser.

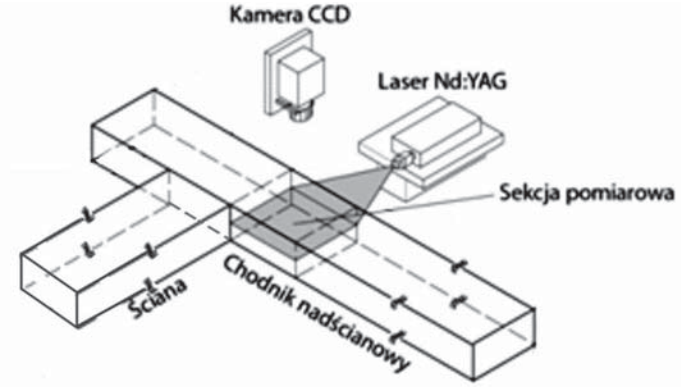

Fig. 2. The measurement station scheme

The movement of particles is registered by the digital camera perpendicular to the light sheet [1,4]. The camera is able to capture each light impulse in separate image frames. The images are divided into small subsections called interrogation areas in size from 8×8 pix to 128×128 pix. The selected interrogation area in the first image frame contains a certain special pattern of particle distribution whose counterpart is searched in the second one. For this purpose an algorithm based on a complex correlation analyses is used. A velocity vector map is obtained by repeating the cross-correlation for each interrogation area over the two image frames. A detailed description of the measurement method can be found in [1, 4, 7].

3. Mathematical model

Classical turbulence modeling is based on Reynolds conception which, for steady and incompressible flows, leads to the equations:

$$\begin{aligned} &\frac{\partial}{\partial x_i}(\rho u_i) = 0 \\ &\frac{\partial}{\partial x_j}(\rho u_i u_j) = -\frac{\partial p}{\partial x_i} + \frac{\partial}{\partial x_j}\left[\mu\left(\frac{\partial u_i}{\partial x_j} + \frac{\partial u_j}{\partial x_i}\right)\right] - \frac{\partial}{\partial x_j}(-\rho\overline{u'_i u'_j}) \end{aligned} \tag{1}$$

where:

u_j — j-component of mean velocity,
p — pressure,
μ — coefficient of dynamics viscosity,
$-\rho\overline{u'_i u'_j}$ — Reynolds stresses.

The most numerous group among the models which close this system of equations includes models which assume occurrence of turbulent viscosity (Boussinesque conception), whereas among them the most frequently used model is the k-ε model by

Harlow and Nakayama. In this model Reynolds stresses are a function of mean rates of deformation:

$$-\rho\overline{u'_i u'_j} = \mu_t\left(\frac{\partial u_i}{\partial x_j} + \frac{\partial u_j}{\partial x_i}\right) - \frac{2}{3}\rho k\delta_{ij} \tag{2}$$

where:

$\mu_t = Ck^2\varepsilon^{-1}$ — coefficient of turbulent viscosity,
k — kinetic energy of turbulence,
ε — rate of dissipation of turbulent energy,
C — constant of the model,
δ_{ij} — Kronecker's symbol.

Kinetic energy of turbulence and the rate of its dissipation are determined on the basis of appropriate transport equations:

$$\begin{aligned}\frac{\partial}{\partial x_j}(u_j k) &= \frac{\partial}{\partial x_j}\left[\left(\nu + \frac{\nu_t}{\sigma_k}\right)\frac{\partial k}{\partial x_j}\right] - \overline{u'_j u'_j}\frac{\partial u_i}{\partial x_j} - \varepsilon \\ \frac{\partial}{\partial x_j}(u_j \varepsilon) &= \frac{\partial}{\partial x_j}\left[\left(\nu + \frac{\nu_t}{\sigma_\varepsilon}\right)\frac{\partial \varepsilon}{\partial x_j}\right] - C_1\frac{\varepsilon}{k}\overline{u'_j u'_j}\frac{\partial u_i}{\partial x_j} - C_2\frac{\varepsilon^2}{k}\end{aligned} \tag{3}$$

where: C_1, C_2, σ_k, σ_ε — the model constants.

In this study two models of turbulence have been tested: the standard k-ε model and its modification the RNG k-ε model. The RNG k-ε model includes the modification to the transport ε-equation, where the effects of rapid rate of strain and streamline curvature are taken into account. The boundary conditions on the rigid walls were set in the form of wall function.

4. The calculation grid

A structured mesh has been generated for the whole computational domain. The mesh was refined in the area of the channels intersection — 1 m before and 2 m after the crossing and near the solid walls. In the later case a solution adaptation technique was use.

The grid convergence was examined by means of the GCI index (grid convergence index). Two grids of total number of elementary cells equal to about 876 000 and 2 950 000 were examined. Maximum and minimum values of velocity vector coordinates for the three cross-sections were compared. The intersections were located at distances of 0.1 m from the corners of crossing. The obtained values of the GCI coefficient for the cross-section in the outlet channel is presented in table 1.

The values of the GCI coefficient rate from 10^{-2}–10^{-3}. The calculations were carried out with the use of a finer grid.

TABLE 1

The GCI coefficients for the cross-section at a distance of 0,1m from the right corner of the channel

Cell number	u_x [m/s] max/min	GCI_u max	GCI_u max	u_y [m/s] max/min	GCI_u max	GCI_u max	u_z [m/s] max/min	GCI_u max	GCI_u max
875 560	16,1577 –1,9353			9,5191 –7,0184			4,7167 –4.7167		
2 953 125	16,2065 –1,9886	$7{,}2\cdot10^{-3}$	$6{,}6\cdot10^{-2}$	9,4922 –7,2117	$6{,}8\cdot10^{-3}$	$6{,}6\cdot10^{-2}$	4,7054 –4,7088	$5{,}7\cdot10^{-3}$	$4{,}0\cdot10^{-3}$

5. The comparison of measurements with calculations

The measurements were conducted for an average flow equal to 9,85 m/s and for a Reynolds number of about 148 600. The measured and computed velocity profile at a distance of 0,1 m from the crossing on the inflow side is shown in Figure 3. The stream-wise and wall-normal components of velocity are presented along two horizontal lines at the ½ and at ¼ height of the duct. In this zone, the calculations are in good agreement with experimental results.

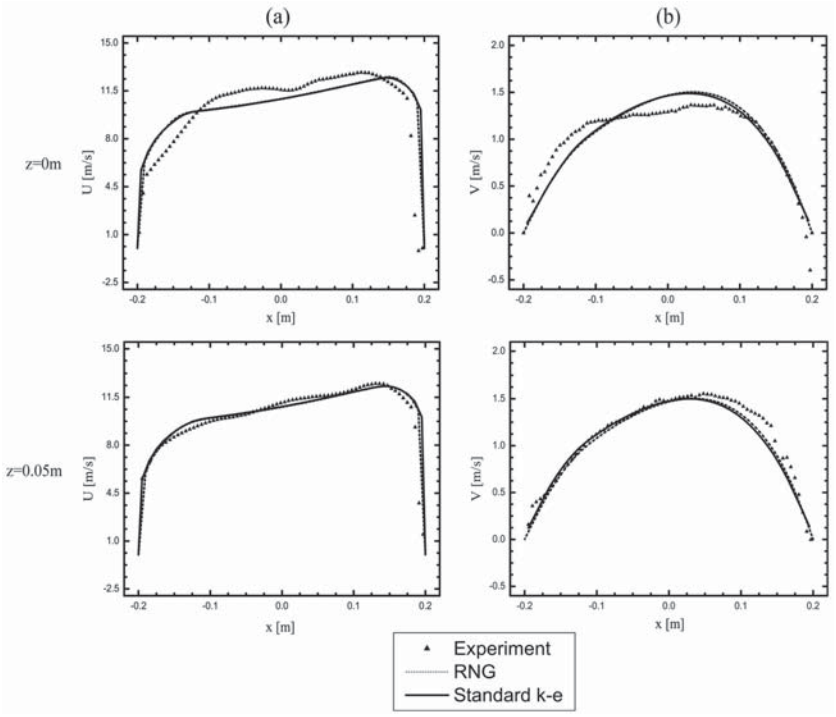

Fig. 3. Flow streamwise (a) and wall-normal (b) velocity component at the middle and ¼ height of the channel at a distance of 0,1 m from the crossing on the inflow side

In the cavity area the measured and numerically determined velocity fields are qualitatively similar however, there are considerable quantitative differences between them. In the Figure 4 are shown the contours of streamwise velocity in three horizontal planes, at ½ and ¼ height of the cavity and at a distance of 0.02 m from the top wall of the duct. A common feature is a narrow stream of air flowing into the cavity taking the shape of the letter C. In the middle of the length of the cavity a virtual stream is divided into roof-adjacent and floor-adjacent parts. This feature of the flow is not verified by measurements.

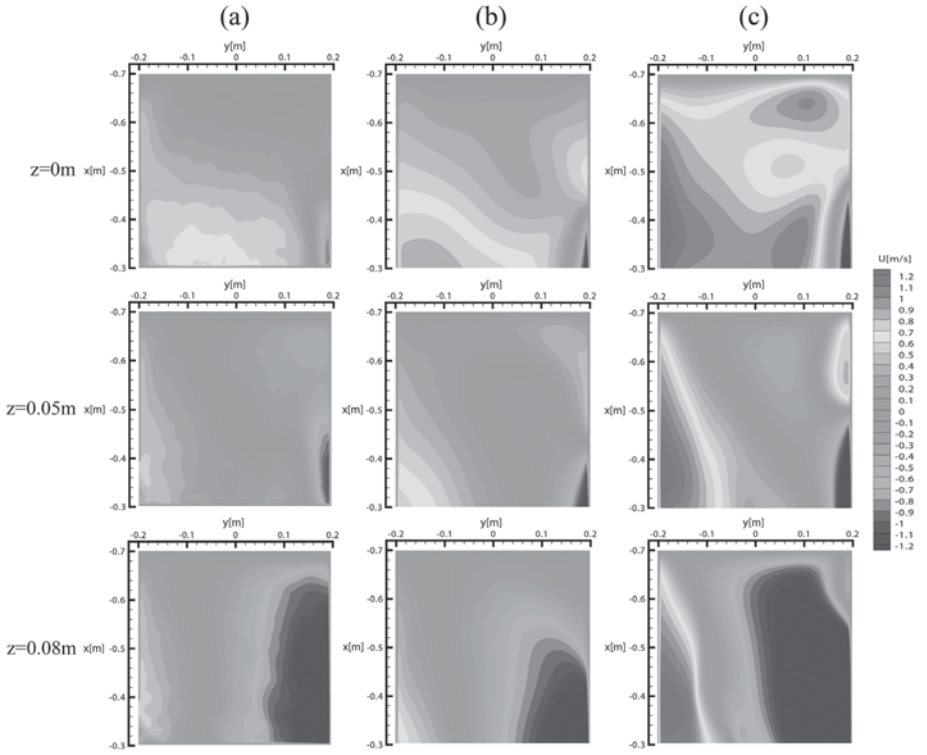

Fig. 4. Contours of stream-wise velocity components in horizontal planes at the middle, ¼ and $^{9}/_{10}$ height of the cavity; experimental results (a), standard k-ε (b), RNG k-ε (c)

In Figure 5 and 6, measured and calculated profiles of a flow streamwise and wall normal velocity components along the three horizontal lines at a distance of 0,1 m and 0,3 m from the left corner of the crossing have been presented. In this domain, the differences between measurements and numerical simulation are significant and for streamwise components are especially large in the zone close to the outside wall of the cavity (for y = 0.2 m). The largest differences for the wall normal components of velocity are observed along the lines at the middle height of the cavity. Both tested models over predict the values of velocities in the cavity zone. This will cause the ventilation to be

overestimated in this area. Much higher values of maximum velocities are predicted especially by RNG k-ε model in comparison to the experimental value. In the cavity zone, better agreement with experiment is reached with the standard k-ε model.

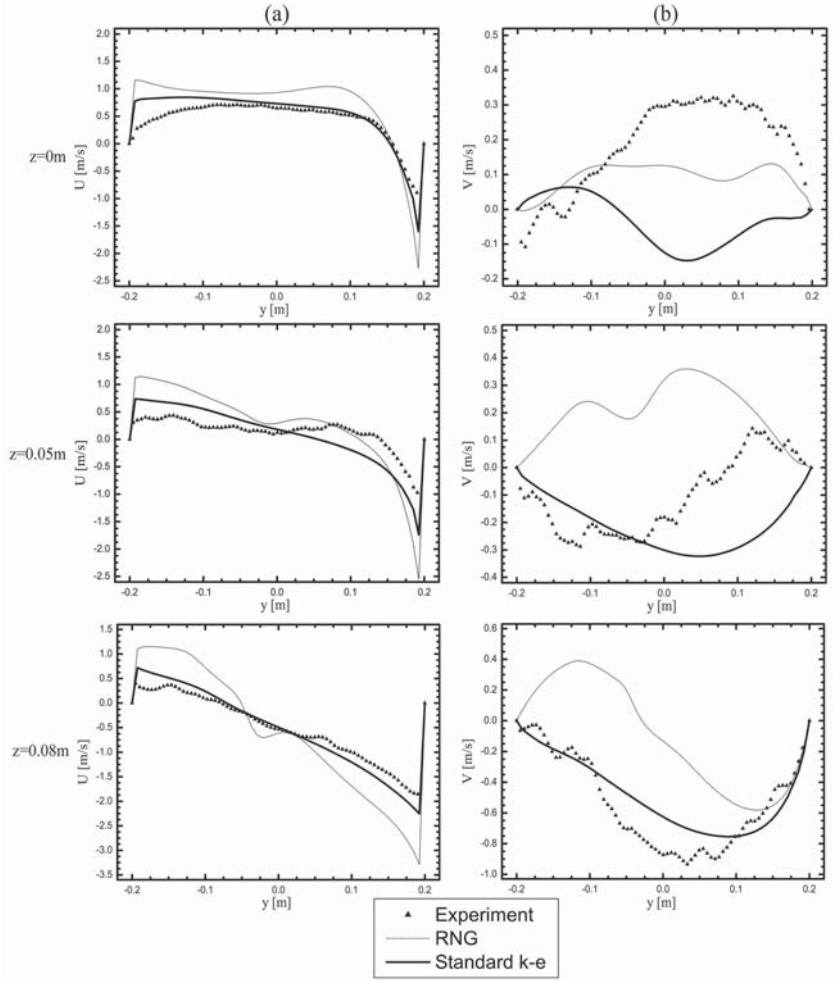

Fig. 5. Flow streamwise (a) and wall-normal (b) velocity component at the middle, ¼ and ⁹⁄₁₀ height of the cavity at a distance of 0,1 m from the left corner of crossing

Velocity distribution at the initial part of the outlet channel is shown in Figure 7. The predicted velocities are in good agreement with the experimental results in the main stream but differ in the separation zone. The shape and length of this zone are better mapped with the RNG k-ε model. The reattachment length calculated with the RNG k-ε model is equal to 81 cm, with the k-ε model equal to 120 cm, whereas the reattachment length determined experimentally is 78 cm long.

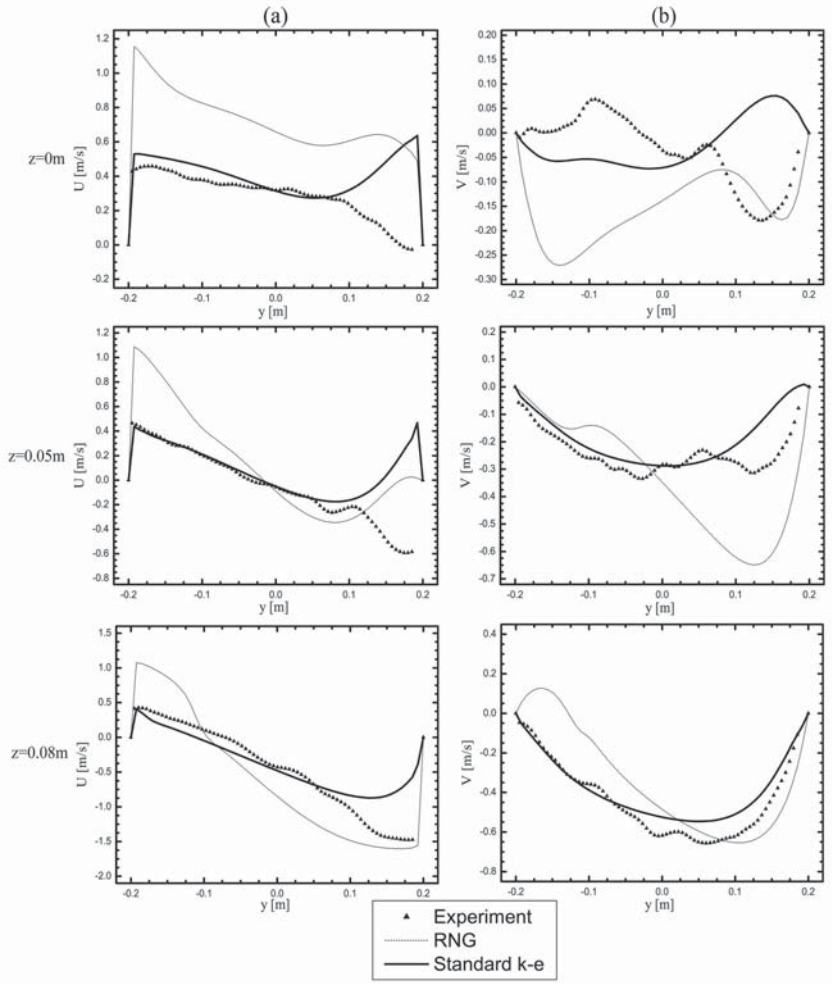

Fig. 6. Flow streamwise (a) and wall-normal (b) velocity component at the middle, ¼ and 9/10 height of the cavity at a distance of 0,3m from the left corner of crossing

6. Summary

None of the developed turbulence models is of a universal character. Thus, the characteristic features of flow determine the choice. The necessity of applying a particular model should be verified experimentally. In spite of the simple geometry of the flow domain, the structure of the generated velocity field in this area is complex. The flow is characterised by such flow features as separation, stream impingement on the wall and strong streamline curvature. In the calculations two models of turbulence were applied: the standard k-ε model and its modification the RNG k-ε model. The k-ε model is most frequently used for solving problems of ventilation. It is used in flows characteristic of isotropic turbulence. The RNG

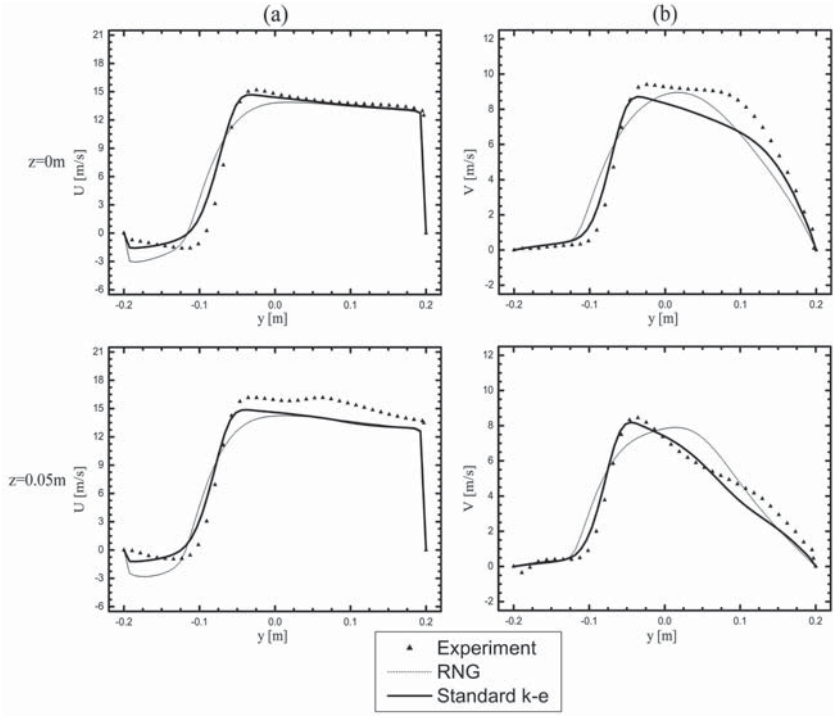

Fig. 7. Flow stream-wise (a) and wall-normal velocity profiles (b) at the middle and ¼ height of the duct in the initial part of the outlet channel (0,1 m from the right corner)

k-ε model is adjusted to flow simulations of low Reynolds numbers where the effects of local small-scale turbulence should be taken into account.

The conducted research allows for the estimation of accuracy with which numerical simulations map the real flow. The largest differences between the measured and calculated velocity field occur in the cavity zone. Both tested models over predict the values of velocities in the cavity zone in comparison to the experimental ones. This will cause the ventilation to be overestimated in this area. Nevertheless, the result obtained using the standard k-ε model are significantly closer to the measured values then those predicted with the RNG k-ε model.

For the cross sections located before (inlet duct) and behind the cross of ducts (outlet duct), the calculations are in quite good agreement with the experimental results, bearing in mind the accuracy needed in ventilation problems.

In the great majority of studies where the CFD methods were used for solving ventilation problems in mines, the standard k-ε turbulence model was applied. The conducted research shows that the quantitative results of numerical simulations can considerably depart from the real values.

The study conducted in the scope of the statute studies (AGH) no. 11.11.100.281 financed by the Ministry of Science and Higher Education.

REFERENCES

[1] Adrian R.J.: *Twenty Years of Particle Image Velocimetry*, Experiments in Fluids, 2005, Vol. 39, Issue 2, p. 159 –169.

[2] Aminossadati S.M., Hooman K. *Numerical Simulation of Ventilation Air Flow in Underground Mine Workings*. 12th US/North American Mine Ventilation Symposium, 2008, p. 253–259.

[3] Branny M., Filek K., Nowak B.: *Kształt pola prędkości w wyrobiskach przewietrzanych wentylatorami wolnostrumieniowymi — symulacja numeryczna przy użyciu lepkościowych modeli turbulencji*. Górnictwo i Geoinżynieria, Akademia Górniczo-Hutnicza im. Stanisława Staszica, Kraków, R.34 (2010), z. 3/1, p. 23–32.

[4] Keane R.D., Adrian R.J.: *Theory of Cross-correlation Analysis of PIV Images*, Applied Scientific Research, 49 (1992), p. 191–215.

[5] Krawczyk J.: *Jedno i wielowymiarowe modele nietsacjonarnych przepływów powietrza i gazów w wyrobiskach kopalnianych. Przykłady zastosowań*. Archives of Mining Sciences, Monografia, nr 2, 2007.

[6] Nawrat S., Kuczera Z., Napieraj S.: *Badania modelowe zwalczania zagrożenia metanowego na wylocie ściany przewietrzanej systemem „U”*. Materiały 4 Szkoły Aerologii Górniczej, Kraków, 10–13 październik 2006, p. 455–466.

[7] Raffel M, Willert C., Wereley S., Kompenhans J.: *Particle Image Velocimetry: Practical Guide*, Springer-Verlag, Berlin, 2007.

[8] Wala A.M., Vytla S., Taylor C.D., Huang G.: *Mine Face Ventilation: a Comparison of CFD Results aAgainst Benchmark Experiments for CFD Code Validation*. Mining Engineering, 2007, no. 10, vol.59, p. 49–55.

[9] Wierzbiński K.: *Modelowanie komputerowe rozkładu parametrów powietrza oraz koncentracji metanu w rejonie skrzyżowania ściany z chodnikiem wentylacyjnym*. 5 Szkoła Aerologii Górniczej, Wrocław 13–16 październik 2009, p. 111–118.